VOL. 17, NO. 19, OCTOBER 2022 ISSN 1819-6608
ARPN Journal of Engineering and Applied Sciences

www.arpnjournals.com

EFFECTS OF TREATMENT PARAMETERS ON ENHANCED OIL PRODUCTION FOR LOWER MIOCENE FORMATION, WHITE TIGER FIELD USING BOX-BEHNKEN DESIGN

Truong Nguyen Huu[1,2] and Wisup Bae[2]
[1]Department of Petroleum Engineering, Faculty of Petroleum, Petrovietnam University, Ba Ria, Viet Nam
[2]Department of Earth and Environmental Sciences, Sejong University, Seoul, South Korea
E-Mail: truongnh@pvu.edu.vn

ABSTRACT

The application of Box-Behnken Design for investigating the effects of treatment parameters including leak-off coefficient, pump rate, proppant concentration end of the job, and injection time, and parameters of the net pay thickness, and porosity of the reservoir on the production performance were discussed. Through analysing the sensitivity of the positive factor influence from high to low on production performance, porosity was the highest factor one, then the pump rate (q, bpm), then the net pay thickness, the proppant concentration end of the job, and then the pumping time. In contrast, when the leak-off coefficient of the permeable thickness was increased from 0.003 ft/min$^{0.5}$ to 0.007 ft/min$^{0.5}$, the production performance was decreased because when the leak-off coefficient increases, the proppant distribution in the created fractures of the net pay thickness will be decreased, leading to poor proppant placement in the net pay thickness, causing to low fracture conductivity.

Keywords: lower miocene reservoir, net present value, box-behnken design, white tiger field.

NOMENCULATURE

NPV = Net present value
Ppf = Pound per feet
EOJ = End of the job
$mm = Million dollars
Ppg = Pound per gallon
Bpm = Barrel per minute
Cum oil = Cumulative oil
API = The American Petroleum Institute
ANOVA = Analysis of Variance
BBD = Box-Behnken Design
SBB = Sintered Ball Bauxite
HSP = High Strength Proppant

1. INTRODUCTION

Currently, hydraulic fracturing is a method of stimulating for most of the oil and gas wells throughout the world and that technique has widely been used to enhance oil and gas production from low, moderate, and high-permeability reservoirs [l]. Hydraulic fracturing stimulation commonly uses a pressurized fracturing fluid injection from the surface of formation to create artificial fractures, which increases the fracture conductivity by creating high propped fracture permeability and wider propped width between the reservoir and the production wellbore [2]. To extract oil from the Lower Miocene reservoir, hydraulic fracturing has been used, and the fracture widths thereof have produced high fracture conductivity, which allows oil from the fractures to easily move to the wellbore. Economides et al. presented a unified fracture design optimization based on proppant mass [1]. Although their study was well conducted, it lacked the optimal surface parameters to maximize the fracture length. Queipo *et al*. [3] developed a method based on the global optimization for hydraulic fracturing treatment design, which considered the Khristianovitch--Gcertsma--de Klerk (KGD), Valko and Economides fracture model [4]. However, the model is rarely used for stimulating oil and gas reservoirs and it does not consider the viscosity of the fracturing fluid as a free design variable. Thus, in most cases, there was a lack of confidence level in analyzing treatment design variables and reservoir parameters because they were always ignored the significance level of treatment parameters and interaction effects between the considered parameters, which may result in low performance in a field operation. To avoid limitations from classical methods, the application of Box Behnken design for analyzing the main parameters and the interaction parameters with the net present value have been presented and discussed. There was a total of 49 tests by using the Box-Behnken design experiment in this study.

2. MATERIALS AND METHODS

2.1 Generality of the Geology

The Lower Miocene reservoir of the White Tiger field is a sandstone formation with high heterogeneity formation, which is separated into two major structures: the Northern dome and Southern dome. The Lower Miocene formation sequence belongs to the Bach Ho Formation where it was developed in an area from 2759 m to 2998 m in depth. The major of the lithological formations included mostly sandstone and siltstone and were cemented by clay or carbonate cement. The sandstones were mostly medium grained. The lithologic composition contains quartz, 40% to 65%, 10-25% of feldspar, 2%-5% of mica, 2%-13% of fragments, and 12-15% of clay or carbonate cement. The production sequence units of the Lower Miocene formation were determined from top to bottom as sequence units 23, 24, and 25. Oil resources were distributed highly in the northern and southern domes. The temperature of the formation was approximately 80 ^{0}C to 100 ^{0}C at producer wells and injector wells by measuring thermometer. The thermal gradient was approximately 3.5 ^{0}C/100m from 1800 m-3600 m in depth. Porosity varied between 0% to 33.5%, with an average of 17.7%, and the permeability of the reservoir ranged between 0.5 mD to 1650 mD by testing the core sample with an average of 239 mD.

Table-1. Characteristic porosity and permeability of the lower Miocene formation.

Centre dome					
Method	**Parameters**	**Permeability, mD**	**Porosity per unit**	**Initial saturation per unit**	**Water saturation per unit**
Core analysis	Average value	276	0.195		0.47
	Variable range	2.5-2500	0.14-0.28		0.20-0.80
Well-log data	Average value		0.182	0.506	
	Variable range		0.14-0.25	0.35-0.71	
Northern dome					
Core analysis	Average value	120	0.19		0.45
	Variable range	2.8-625	0.14-0.24		0.28-0.75
Well-log data	Average value		0.189	0.522	0.478
	Variable range		0.14- 0.25	0.35-0.84	0.16-0.65

2.2 Historical Production of the Lower Miocene Formation, White Tiger Field

Until July 1, 2015, oil production from the Miocene formation had been obtained 9,213,652 tons (t) under a water cut of 47.1%. Until July 1, 2015, the number of wells of the lower Miocene reservoir of the White Tiger field comprised 08 producer wells (including 18 stopped wells), and 15 injector wells, 1 stopped well, and 26 abandoned wells. In 2015, the average oil production rate of each producer well was 46 t/day, where the liquid production rate was 92 tons/day with an average water cut of 50.1%, the gas-oil ratio factor was 125 m^3/t, the received water 474 m^3/day. The compensation production factor was 60.4%. The amount of oil production at the beginning of exploitation was 9,214×10^3 t, the liquid production was 17,409×10^3 t, the amount of water injected was 14,673×10^3 t, with a recovery factor of 0.198. Between the years 1987 and 1997, water was injected into the formation through one injector well with an injection rate within 27×10^3 m^3/year and 128×10^3 m^3/year. In the year 1997, another injector well was added for the water flooding system. The water injector wells were maintained the production rate of producer wells by increasing the reservoir pressure. The volume of water injected declined slightly in the last three years because the reservoir pressure of the formation had been reached hydrostatic pressure. Currently, the Miocene formation consists of 7 injector wells, which were used for injecting water into the formation within pump pressure 4.2 MPa and 24.2 MPa. Water was appeared in the liquid production after three years of exploitation. In 1990, the water cut was 19.2% and it remained at the same level until 1993. In 2000, the water cut was climbed up again to 43.7% in the year 2000 after changing the number of producer wells to gas-lift wells without using a compressor. Since 1997, it has been exploited by gas lift using a compressor. By the year 2015, the water cut level had been reached 50.1%. During the exploitation of the eastern wing of the structure, it was noticed the appearance of marginal water pressure, but it was not enough to prevent the reduction of reservoir pressure energy in the regional production.

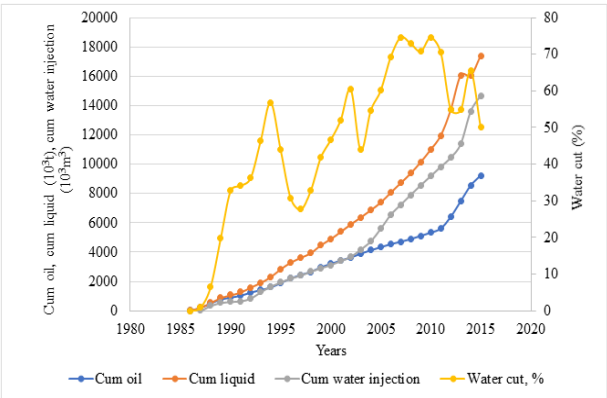

(1a)

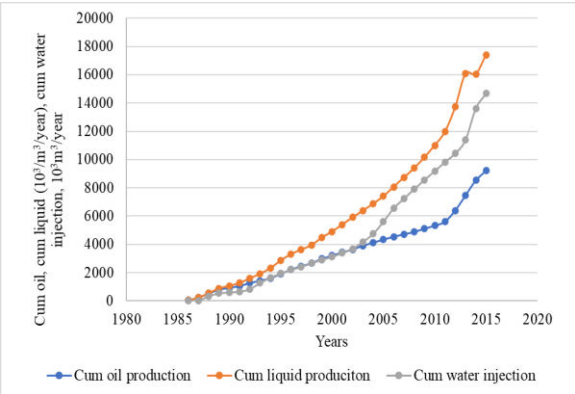

(1b)

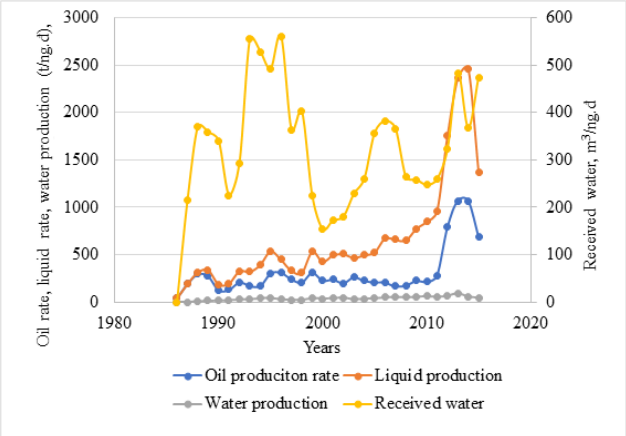

(1c)

Figure-1. Technological performance indicators of the Miocene formation, White Tiger Field.

2.3 Northern Dome Structure

Until July 1, 2015, the oil reservoirs at the Northern dome had been produced 4,286×10^3 t with a recovery factor of 0.271. The dome structure was separated into these blocks, and it was initially produced in November 1986. Oil production was obtained 187×10^3 t in the year 1989, and then oil production was declined quickly to 88×10^3 t by the year 1990 and 93×10^3 t by the year 1991 due to an increase in water cuts and the number of natural producer wells were sopped. Adding new producer wells and changing the natural production wells to artificial lift producer wells by the year 1995, the oil exploitation was reached within 120 and 170×10^3 t. In the years 1995 and 1997, oil production was up to 250×10^3 tons and 265×10^3 tons, respectively due to added five producer wells with high production rate. In 1998, oil production was decreased to 176×10^3 t due to water cuts increased and natural producer wells stopped. Between the years 1999 and 2002, the oil production increased up to 276×10^3 tons where the highest oil production was reached in 1999, and then it gradually declined to 152×10^3 tons in the year 2002. During this period, it had been carried out a lot of works such as operating producer wells in filled wells and changed producer wells from basement formation to Miocene formation, changed producer wells from natural production to gas-lift wells, treated near wellbore areas for producer wells. Water injection was carried out for 3 injector wells since 1988. The annual amount of water volume injected was uneven by operating producer wells at various times with different recovery rates of fluid production according to the blocks. However, the current water injection was ensured to maintain the reservoir pressure of the regional production, which was higher than the saturated pressure.

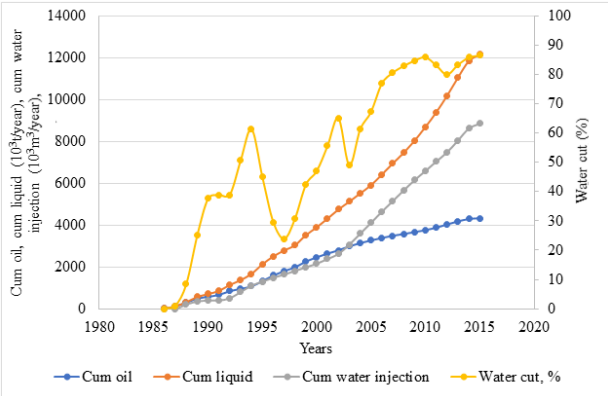

(2a)

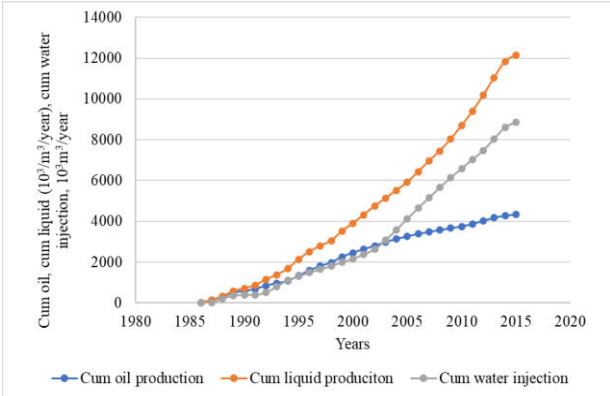

(2b)

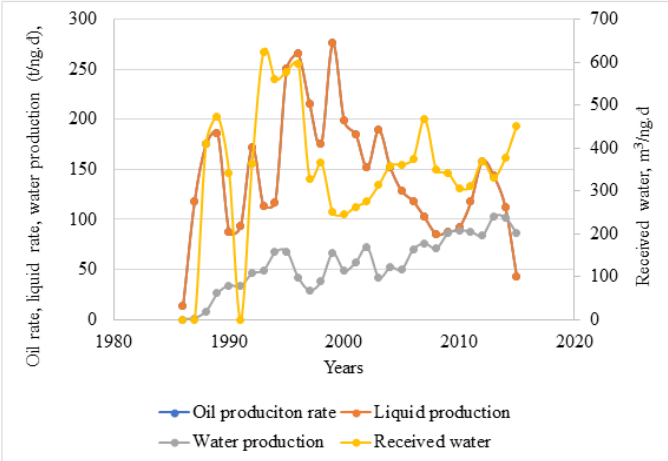

(2c)

Figure-2. Technological performance indicators of the Northern dome structure of the lower Miocene formation, White Tiger Field.

2.4 Central Dome Structure

Oil reservoir in the central dome structure was initially exploited since 1986. The water injection into the formation to maintain reservoir pressure was initiated since 1987. After one year of producing oil, oil production was peaked at 120×10^3 tons in the year 1988, and then it was followed by a decline in oil production to 30×10^3 tons in the year 2000 because it was increased in water cut from liquid production and stopped injector wells. In 2001, by adding one new producer well to the drilled well and the near wellbore treatment of the well, the oil production was climbed up to 52×10^3 tons, the water cut from the liquid production was declined from 43.7% to 33.1%. In the year 2002, the production was 48×10^3 tons with the water cut 32.1%. The cumulative production was obtained $2{,}704\times10^3$ tons until 1, 2015, where the oil recovery factor was 0.178. Oil formation of the central dome structure was divided into 2 zones including 1 and 2. Zone 1 was located to the west of the fault along well 127 and well 145. Through the distribution of water saturation according to the production layers, the historical production matching was obtained based on the calculated model, and geology analysis was noticed that the eastern wing was conducted with water flooding by injector wells to increase the reservoir pressure energy of producer wells, which had a higher oil recovery factor than the western wing. Production layers such as 230 and 231 were the best exploitation. Through the study shows that apart from oil reserves can be fully exploited by these wells produced from other formations. Production layer 232 had a medium oil recovery factor. Some individual areas in the northern and west - south can be exploited by reoperating wells. Oil reserves of sequence units 23 and 24 were 417.3×10^3 t.

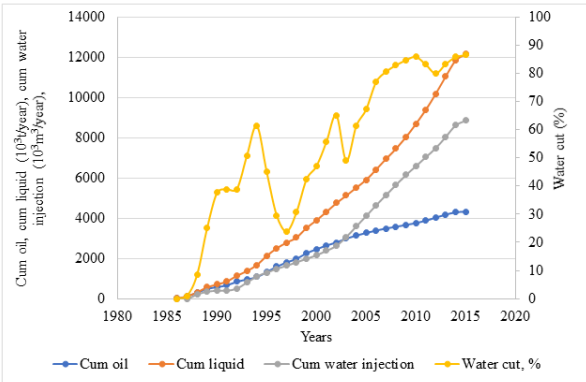

(3a)

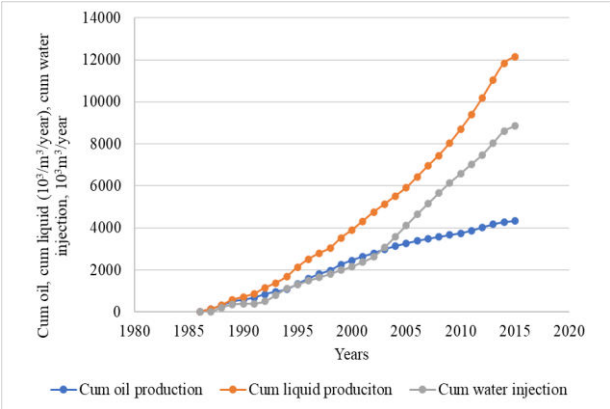

(3b)

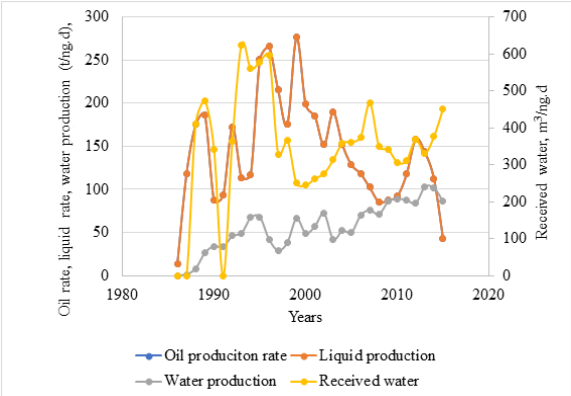

(3c)

Figure-3. Technological performance indicators of the central dome structure of the lower Miocene formation, White Tiger field.

3. STATEMENT OF RESERVOIR PRESSURE ENERGY OF LOWER MIOCENE FORMATION, WHITE TIGER FIELD

3.1 The Northern Dome Structure

The initial reservoir pressure within the northern dome was measured at the beginning of the production phase and it was moved to the positional oil-water contact at a reservoir pressure of 29.6 MPa with 2971 m in depth. The oil body was divided into three blocks including I, II, and III, based on the various effects of pressure from injector wells and the marginal water pressure from producer wells. Block I consists of wells such as 163, 169, 170, 171, 174, 179, 183, 187, 193, 198, 1117, 1130. During the starting production phase, the reservoir pressure was decreased sharply. The water injection was started in April 1988 to build up the reservoir pressure and stabilized. Pressure between 26 MPa and 28 MPa. At the end of 1996, after stopping the injection of water, the oil body was continued to be exploited under decreasing reservoir pressure. In 2002, the reservoir pressure was measured producer well which was decreased to 20.5-20.7 MPa (saturated pressure was 20.4 MPa). In October 2002, the water injection was restarted to maintain the reservoir pressure of these producer wells. Block II has producer wells such as 182, 186, 1121, 1136, which were produced under the influence of water pressure at boundaries. Oil Production from producer wells is located in the central block, where the reservoir pressure at the end of the production period has decreased to only 27 MPa. Block II comprised these wells such as 195, 1202, 1804, 1806, 1815, 1816, 1817, 1818, 1820, 1917. Between 1987 to 1994, only I injector well was used for maintaining reservoir pressure for the producer wells. During this period, the reservoir pressure was declined insignificantly to 25.7 MPa at the end of the year· 1994. An increase in oil production was caused by a decrease in reservoir pressure sharply. In May 1996, the reservoir pressure was measured to convert pressure 21.8 MPa at the boundary oil-water contact position with 2,971 m in depth. In May 1996, the water injection for this period was initiated to increase the reservoir pressure and maintain pressure for the stages of exploitation. In August 2002, the reservoir pressure was measured and varied within 24.1 MPa and 24.5 MPa, this magnitude of the reservoir pressure allowed to produce a high production rate from producer wells, and 2 wells were continued to produce under natural production. The reservoir pressure behavior of producer wells in the Northern dome was shown in Figure-4.

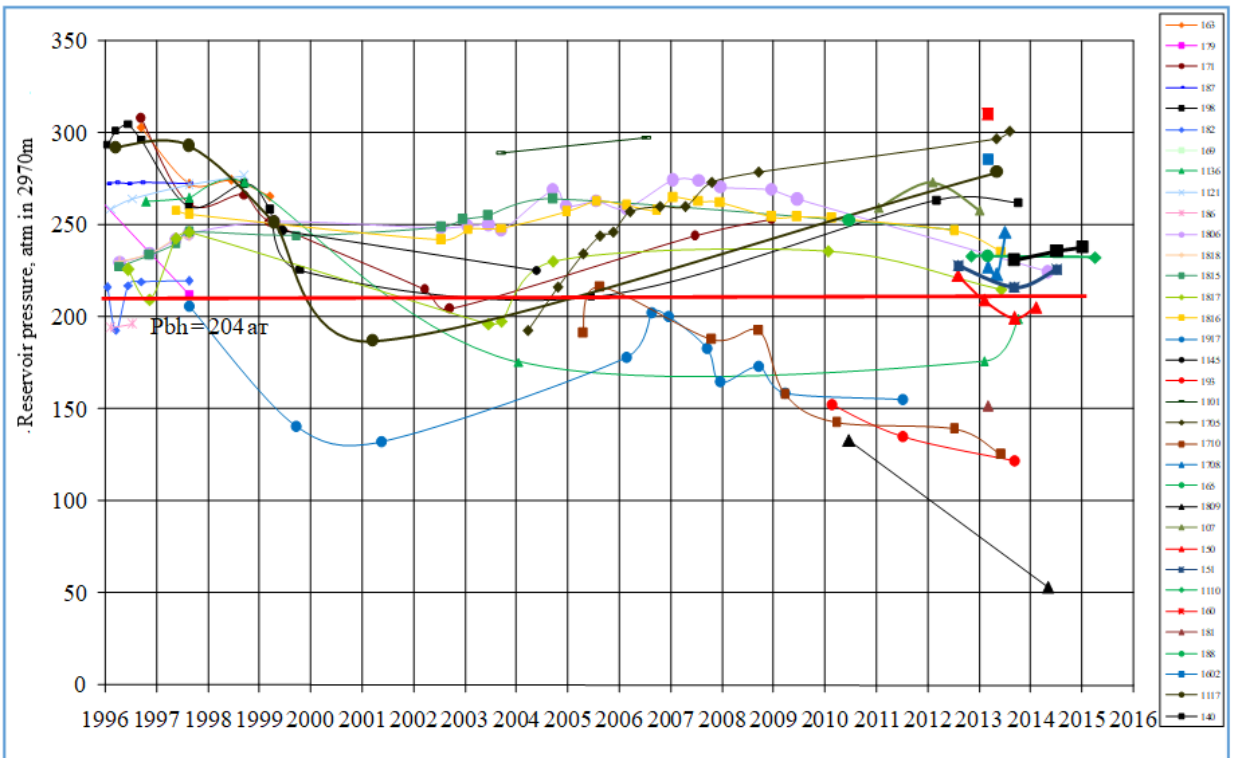

Figure-4. Statement of reservoir pressure for producer wells in the Northern Dome of the lower Miocene Formation, White Tiger field.

3.2 The Central Dome Structure

The initial reservoir pressure of the oil body of the central dome was measured in the early stage of oil exploitation and was moved to the positional oil-water contact at a reservoir pressure of 28.1 MPa at 2,821 m in depth. According to the statement of the reservoir pressure during producing extraction, the oil body was divided into two separate regions including western region and eastern region. The western region of the oil body was noticed by poor connectivity at the boundary, with the increase of oil recovery, the reservoir pressure was tended to decline during producing exploitation until water was initially injected in July 1987. By conducting water injected into the reservoir and adding new producer wells to enhance oil recovery, the reservoir pressure was gradually increased, and it was maintained between 25 MPa-30 MPa. Since 1998, the current production compensation factor and the cumulative production compensation had been exceeded 100%, resulting in a decrease in the reservoir pressure in the southern areas of the oil body, the pressure had been decreased significantly to 12 MPa. This was proved very poor hydraulic connectivity among this area with producer wells and injector wells of the oil body. The eastern region of the oil body was supported by marginal water pressure. However, the energy of the marginal water was not large enough, because the reservoir pressure at the wells was reduced to 19.8 MPa- 20.7 MPa, although still higher than the saturated pressure (14.6 MPa), but already lower than the initial reservoir pressure (28.1 MPa). The reservoir pressure energy statements of the producer wells of the central dome are shown in Figure-5.

VOL. 17, NO. 19, OCTOBER 2022 ISSN 1819-6608
ARPN Journal of Engineering and Applied Sciences

www.arpnjournals.com

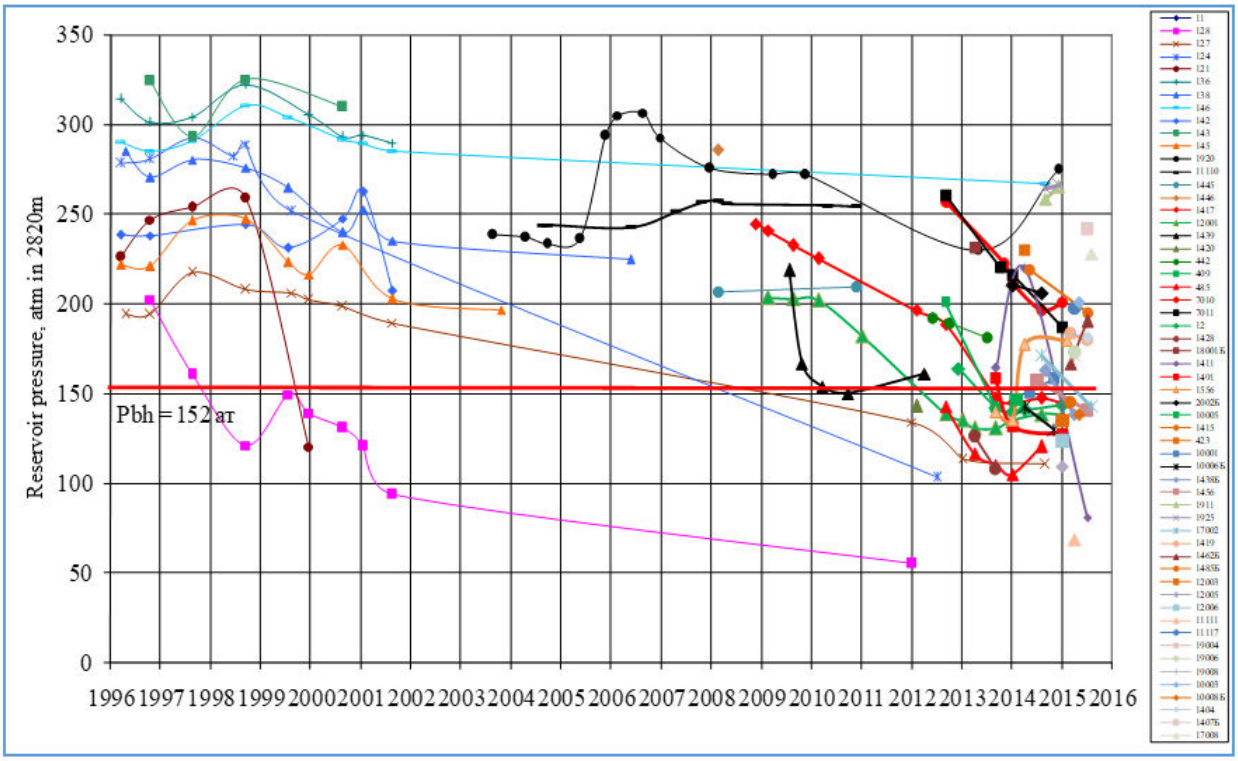

Figure-5. Reservoir pressure energy statement of producer wells of the Central dome of Lower Miocene formation, White Tiger field.

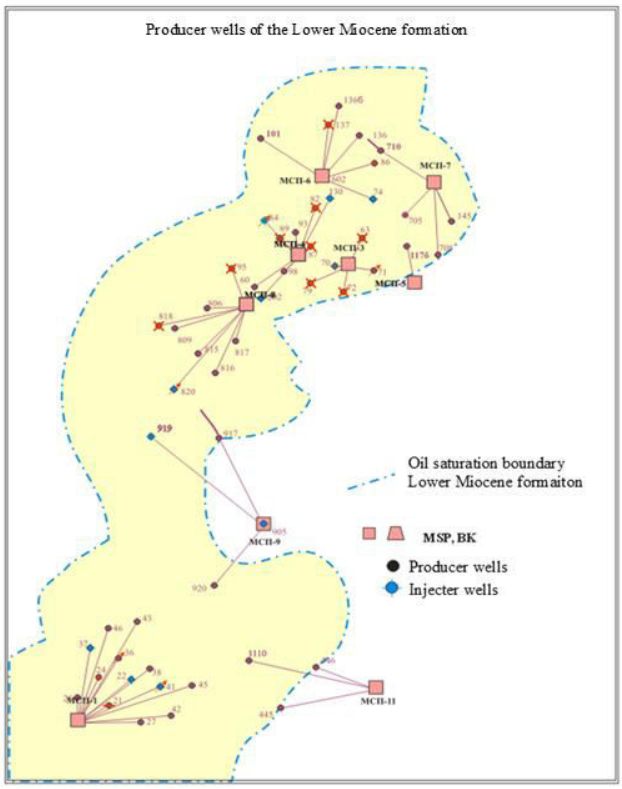

Figure-6. Producer locations of lower Miocene formation, White Tiger field.

4. THE NET PRESENT CALCULATIONS AND MODELING

Step-by-step computational procedure for the calculated NPV and analyzing the influence of treatment parameters on NPV as follows:

- Reservoir properties (reservoir thickness, reservoir porosity, reservoir pressure, in-situ stress)
- Select treatment design parameters such as leak-off coefficient (ft/min), pump rate (bpm), injection time (minutes), and proppant concentration EOJ (ppg), reservoir porosity, and reservoir thickness. Select the appropriate design of the experiment and use the modeling design of the experiment (Modde 5.0) [4]
- Select the appropriate fracture propagation model (PKN-C or GDK-C model) [5] based on formation characteristics and pressure fall-off behavior during the calibration treatment test.
- Select the appropriate proppant type based on proppant strength and formation embedment characteristics. Select fracturing fluid systems most applicable to the formation are treated. Determine the fracture length, width, proppant mass requirement, and fluid volume requirement from material balance. Construct the inflow performance relationship (IPR) curve and outflow performance relationship (OPR) to determine the flowing bottom hole pressure (P_{wf}, psi) and production rate operation (q, STB/day). Integrated production decline curve to obtain the cumulative oil production (bbls) over an operation three-year period.

- Calculate the fractured well net present value and non-fractured well net present value based on the assumed discount rate.
- Calculate the total treatment cost comprising proppant cost, fluid cost, hydraulic power cost, and miscellaneous items cost.
- Calculate the net present value (NPV) by subtracting the total treatment cost from the discount revenue.
- Analyze the effect of main and interaction of treatment parameters and porosity of the reservoir, permeability of the reservoir.
- Sensitivity analyzes the impacts of leak-off coefficient (ft/min$^{0.5}$), pump rate (bpm), injection time (minutes), and proppant concentration EOJ (ppg), reservoir porosity, and reservoir thickness on the net present value (NPV).

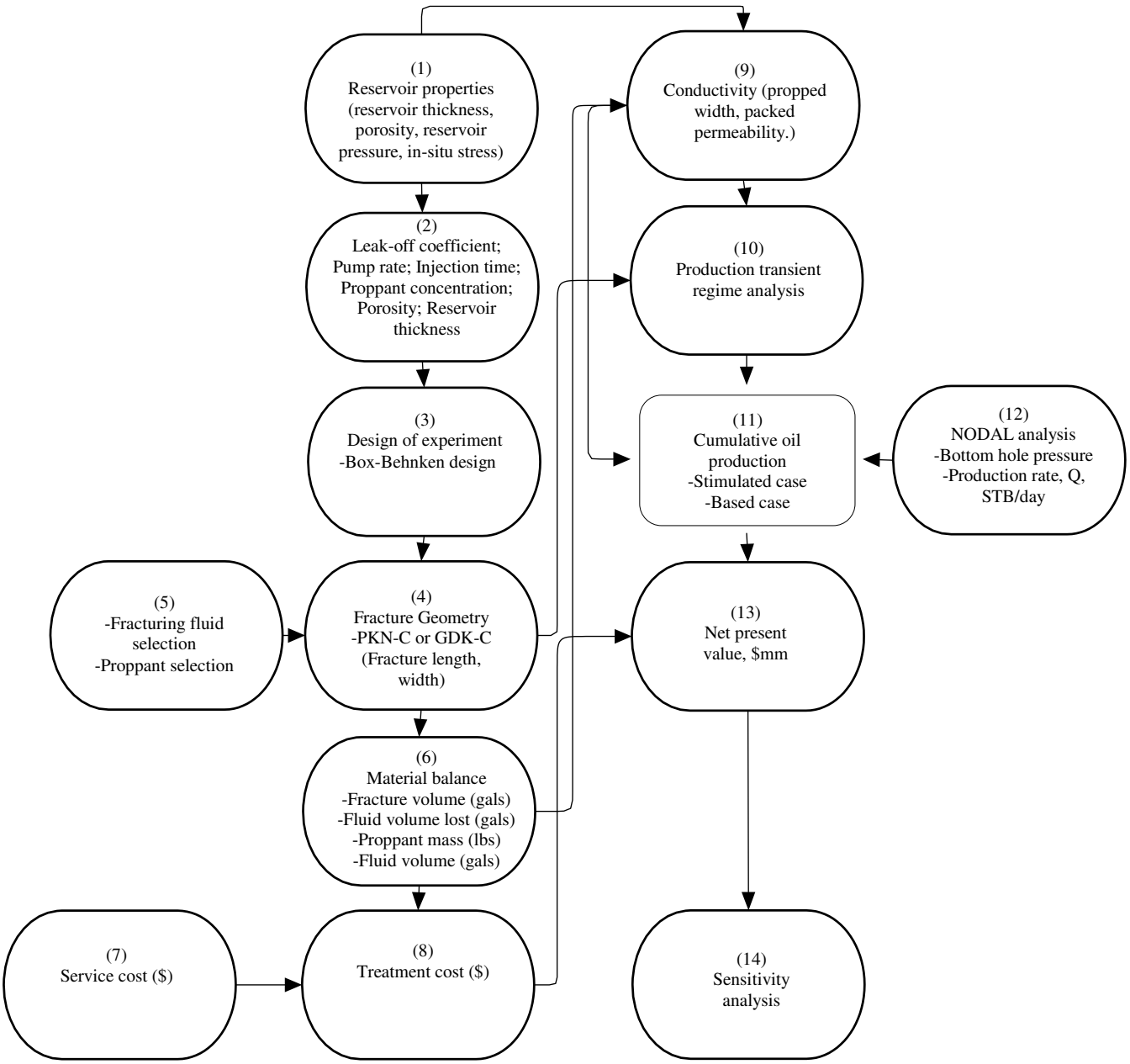

Figure-7. Integrated model for enhanced oil production by hydraulic fracturing [24].

4.1 Box-Behnken Design

The design of the experiment has been widely used to optimize the analytical method due to several benefits because of a decrease in the number of experiments works that need to be done, which results in reducing economic costs. One of the efficiently alternating designs of the experiment was the Box-Behnken Design. The BBD is commonly used for fitting second-order models. The total number of runs for BBD is N= 2k(k-1) +C_0 (where k is the number of factors and C_0 is the number of centers). The advantage of BBD is that it is high efficiency in comparison with another design of experiment such as central composite design in all cases [6, 7, 8]

4.2 Data Description

The six parameters consist of leak-off coefficient (ft/min$^{0.5}$), pump rate (bpm), proppant concentration, end of the job (ppg), injection time (minutes), and porosity of the reservoir (%) and reservoir thickness (ft) that have been studied and the influence of those on the net present value (NPV). Ideally, the first four variables are designed on the surface and two parameters of the reservoir are uncontrolled on the surfaces which are influenced by the NPV. In the field, six parameters ranged between the lower and upper bounds are as follows:

300 ft< hp < 230 ft: Ngoc *et al*., [9]

14% < Por < 24%: Ngoc *et al*., [9]

6 ppg< P_c<10 ppg: industry practice and Meng and Brown [10]

60 minutes< t<90 minutes: The upper bound 90 minutes was chosen so that the optimum value of injection time is never constrained by the injection time [10]

16 bpm <q<30 bpm: Rahman *et al*., [11]. The surface pressure requirement was below the working rating pressure of the equipment and the formation is not breakdown due to the excessive net pressure. The bottom hole treating pressure is below the burst pressure resistance of the tubing.

0.003 ft/min$^{0.5}$<C_l<0.007 ft/min$^{0.5}$: Jain *et al.*, [12]

These variables and their levels for BBD used in this study are shown in Table-3. Using the relation of variable levels in Table-3, the coded variables and the actual variables for each design matrix were determined as given in Table-4.

5. RESULTS AND DISCUSSIONS

Table-2 shows the upper bound and lower bound for a case study of the lower Miocene reservoir of the center of variables with the BBD for 49 runs as shown in Table-3.

Table-2. Reservoir and well data [17].

Parameters	Values
Reservoir drainage area	1 94 acres
Reservoir depth	9,612 ft
Net pay thickness	30 ft-230 ft
Reservoir porosity	14%-28%
Reservoir permeability	2.7 mD
Initial reservoir pressure	3,960 psi
Reservoir temperature	221 ^{0}F
Oil saturation	63%
Total compressibility	1.45×10^{-5} psi^{-1}
Minimum horizontal stress	5,072 psi
Young's modulus	3×10^6 psi
Poisson's ratio	0.25
Wellbore radius	0.25 ft
Formation volume factor	1.4 factor
Reservoir fluid viscosity	1.074 cp
Tubing size	2-7/8 in
Proppant type: HSP, Sintered Ball Bauxite (SBB), 16/30, Specific gravity 3.56.	

Table-3. Six variables and their levels for BBD.

	Coded variable			
		Low	Center	High
Variable	Symbol	-1	0	1
Leak-off coefficient, ft/min$^{0.5}$	X1	0.003	0.005	0.007
Pump rate, q, bpm	X2	16	23	30
Injection time, t, minutes	X3	60	75	90
Proppant concentration EOJ, P_c, ppg	X4	6	8	10
Net pay thickness, hp, ft	X5	30	130	230
Porosity of reservoir, Por, %	X6	14	19	24

VOL. 17, NO. 19, OCTOBER 2022 ISSN 1819-6608
ARPN Journal of Engineering and Applied Sciences

www.arpnjournals.com

Table-4. Independent variables and results for NPV design by BBD.

Run	Coded level of the variables						Actual level of the variables						Response	
	C_l	q	t	P_c	Por	hp	C_l, ft/min$^{0.5}$	q, bpm	t, minutes	P_c, ppg	Por, %	hp, ft	$mm NPV	Cum oil 10^3, bbl
1	-1	-1	0	-1	0	0	0.003	16	75	6	19	130	69	1,074.7
2	1	-1	0	-1	0	0	0.007	16	75	6	19	130	52.4	918.8
3	-1	1	0	-1	0	0	0.003	30	75	6	19	130	87	1,242
4	1	1	0	-1	0	0	0.007	30	75	6	19	130	66.7	1,055
5	-1	-1	0	1	0	0	0.003	16	75	10	19	130	75.3	1,133.2
6	1	-1	0	1	0	0	0.007	16	75	10	19	130	56.8	961.31
7	-1	1	0	1	0	0	0.003	30	75	10	19	130	95.3	1,318.5
8	1	1	0	1	0	0	0.007	30	75	10	19	130	72.5	1,109.6
9	0	-1	-1	0	-1	0	0.005	16	60	8	14	130	56.4	950.4
10	0	1	-1	0	-1	0	0.005	30	60	8	14	130	70.6	1,084.7
11	0	-1	1	0	-1	0	0.005	16	90	8	14	130	59.3	977.85
12	0	1	1	0	-1	0	0.005	30	90	8	14	130	75.3	1,129.6
13	0	-1	-1	0	1	0	0.005	16	60	8	24	130	62.4	1,017.9
14	0	1	-1	0	1	0	0.005	30	60	8	24	130	79	1,172.9
15	0	-1	1	0	1	0	0.005	16	90	8	24	130	65.7	1,049.4
16	0	1	1	0	1	0	0.005	30	90	8	24	130	84.5	1,225.5
17	0	0	-1	-1	0	-1	0.005	23	60	6	19	30	23.2	316.31
18	0	0	1	-1	0	-1	0.005	23	90	6	19	30	26.6	348.4
19	0	0	-1	1	0	-1	0.005	23	60	10	19	30	24.8	331.61
20	0	0	1	1	0	-1	0.005	23	90	10	19	30	28.9	369.52
21	0	0	-1	-1	0	1	0.005	23	60	6	19	230	94.7	1,643.7
22	0	0	1	-1	0	1	0.005	23	90	6	19	230	98.2	1,677.1
23	0	0	-1	1	0	1	0.005	23	60	10	19	230	102.8	1,721.2
24	0	0	1	1	0	1	0.005	23	90	10	19	230	107.2	1,762.7
25	-1	0	0	-1	-1	0	0.003	23	75	6	14	130	74	1,115.4
26	1	0	0	-1	-1	0	0.007	23	75	6	14	130	56.9	955.91
27	-1	0	0	1	-1	0	0.003	23	75	10	14	130	80.7	1,177.7
28	1	0	0	1	-1	0	0.007	23	75	10	14	130	61.6	1,001.3
29	-1	0	0	-1	1	0	0.003	23	75	6	24	130	83	1,208.9
30	1	0	0	-1	1	0	0.007	23	75	6	24	130	63	1,024.2
31	-1	0	0	1	1	0	0.003	23	75	10	24	130	90.9	1,282.2
32	1	0	0	1	1	0	0.007	23	75	10	24	130	68.5	1,076.4
33	0	-1	0	0	-1	-1	0.005	16	75	8	14	30	21.4	298.66
34	0	1	0	0	-1	-1	0.005	30	75	8	14	30	26.7	348.31
35	0	-1	0	0	1	-1	0.005	16	75	8	24	30	24.6	327.78
36	0	1	0	0	1	-1	0.005	30	75	8	24	30	31	387.37
37	0	-1	0	0	-1	1	0.005	16	75	8	14	230	83.7	1,528.8
38	0	1	0	0	-1	1	0.005	30	75	8	14	230	106.1	1,741.6
39	0	-1	0	0	1	1	0.005	16	75	8	24	230	92	1,627
40	0	1	0	0	1	1	0.005	30	75	8	24	230	117.7	1,869.9
41	-1	0	-1	0	0	-1	0.003	23	60	8	19	30	27.4	353.01
42	1	0	-1	0	0	-1	0.007	23	60	8	19	30	22.1	305.38
43	-1	0	1	0	0	-1	0.003	23	90	8	19	30	32.4	399.51
44	1	0	1	0	0	-1	0.007	23	90	8	19	30	25.1	333.7
45	-1	0	-1	0	0	1	0.003	23	60	8	19	230	115.9	1,843.2
46	1	0	-1	0	0	1	0.007	23	60	8	19	230	88.5	1,585.2
47	-1	0	1	0	0	1	0.003	23	90	8	19	230	121.9	1,899.4
48	1	0	1	0	0	1	0.007	23	90	8	19	230	91.3	1,613.2
49	0	0	0	0	0	0	0.005	23	75	8	19	130	70.7	1,091.4

The step by step calculating NPV of the fractured well and nonfractured well have been presented in Figure-7. The net present value over an operation of a production period of three years was selected as the response variable

to evaluate the oil production performance. It was noticeable that the maximum NPV was obtained when the value of total treatment cost was lowest. The discount rate of 10% yearly during 3 years of production life. The production data in three years based on the operating production rate with bottom hole flowing pressure of 3,500 psi from the inflow performance relationship [13] and tubing performance relationship [14] comprised only oil production and the percentage of water cut of 6%. Economic data including the average price of sweet light oil of the White Tiger field was 60 $/bbl. The total treatment cost depends on the pump rate and bottom hole treatment pressure when the pump cost is 3.25 $/HHP. In addition, the material for hydraulic fracturing is a proppant cost, 0.4 $/lb and fracturing fluid cost of 1 $/gallon. The jack-up rig cost and the vessel cost are considered 75,000 $/day and 15,000 $/day, respectively. The result showed that the thickness of the reservoir is significantly affected by the NPV. Based on Table-3, the highest NPV was identified in the case of 47 under the treatment parameters of leak-off coefficient of 0.003 ft/min$^{0.5}$, pump rate of 23 bpm, proppant concentration end of the job of 10 ppg, injection time of 75 minutes, and two parameters of the reservoir including porosity 19% and reservoir thickness 230ft. Based on the results of the analysis of variance, goodness-of-fit and adequacy of the models have been listed in Table-5. The determination of coefficient (R^2=0.999) was displayed in ANOVA of the quadratic regression model. The value of the adjusted coefficient determination (Adjusted R^2=0.998) also the table deflected that the model was highly significant with 95% confidence level. Similarly, a very low value of 0.0001 of the coefficients of the residual standard deviation is clearly noticeable that the high degree of precision and a good deal of reliability of the experimental values and especially the one related to the power of prediction, Q=0.996.

5.1 The Main and Interaction Effect Plots

Figure-8 shows the effect plots of the variables on the NPV. It is noticeable that the graph is separated into two regions, consisting of the region below zero and the region above zero. The first region is shown the factors of the variables, and the interaction variables are below zero, including XI, XI.XI, X2.X2, X5.X5, X1.X6, X2.X5, X2.X6, X5.X6, which are predicting the decrease level of the NPV when these variables change. The second region is above zero, where the factors of the variables and interaction variables present the positive coefficients, namely, X2, X3, X4, X5, X6, XI.X1, X3.X3, X4.X4, X2.X3, X2.X4, X3.X4, X3.X5, X3.X6, X4.X5, X4.X6 which define the NPV level to analyze the Pareto chart in Figure-8. To present the effect plots; the modeling design of experiment software is used to analyze coefficients, the levels of the variables, and interaction variable effects on the NPV (Figure-8). For analyzing the Pareto chart presented in Figure-8. Thus, the reservoir thickness parameter with the coefficient factor of 37.7417 influences significantly on the NPV.

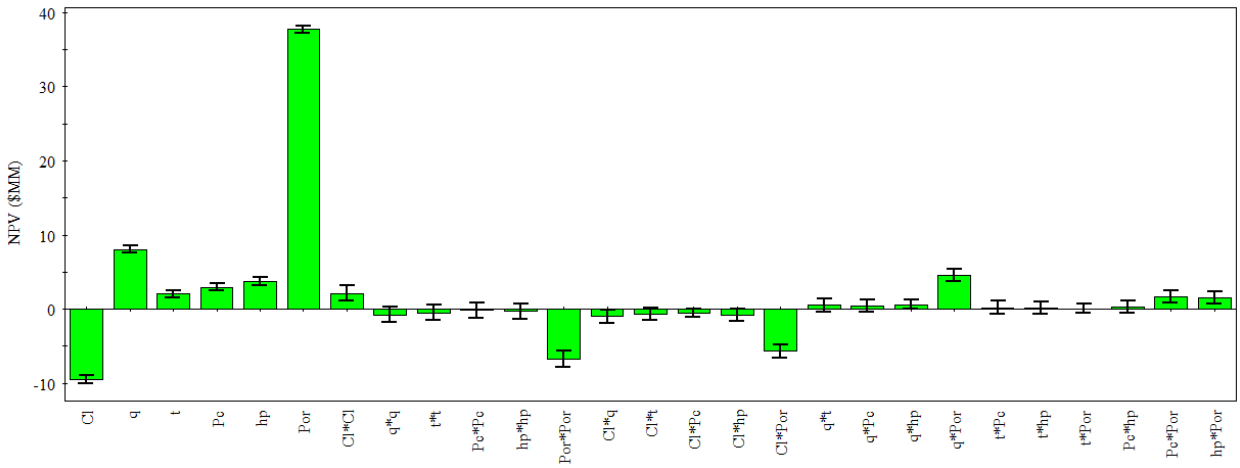

Figure-8. The effect plots of variables on the NPV.

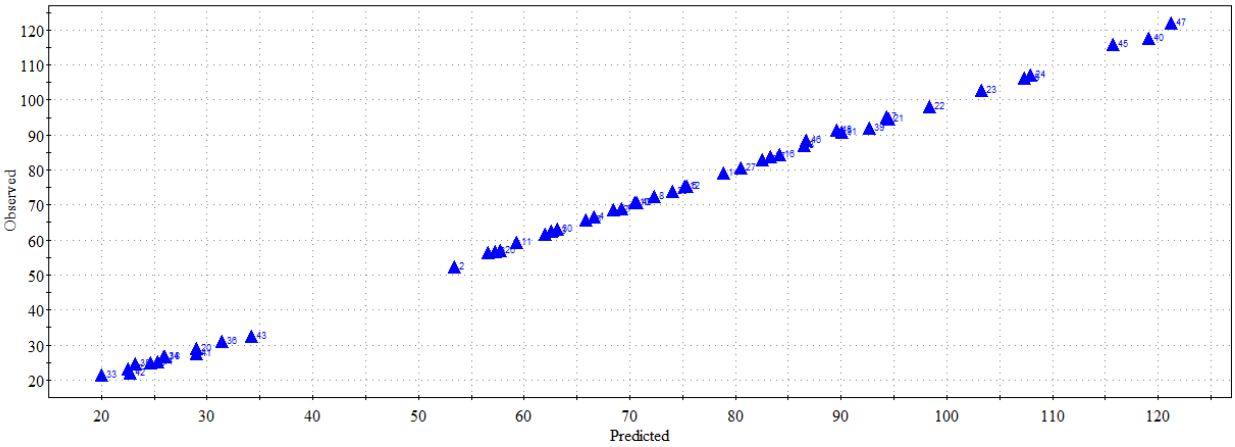

Figure-9. Observed NPV versus predicted NPV.

5.2 The Effect of Leak-Off Coefficient on Net Present Value (NPV)

Figure-10 presents the effect of the leak-off coefficient versus the NPV. Leak-off coefficient was investigated within 0.003 ft/min$^{0.5}$ to 0.007 ft/min$^{0.5}$ [12]. From this figure, there is a slight nonlinear relationship between the leak-off coefficient and the NPV. Based on this graph, the NPV decreases from over 82 $mm to over 63 $mm as the leak-off coefficient increases from 0.003 ft/min$^{0.5}$ to 0.007 ft/min$^{0.5}$. Between 0.003 ft/min$^{0.5}$ and 0.005 ft/min$^{0.5}$ of leak-off coefficient, the NPV was considerably decreased from nearly 85 $mm to approximately 70 $mm when the NPV was decreased by nearly 15 $mm. Between 0.005 ft/min$^{0.5}$ to 0.007 ft/min$^{0.5}$ of leak-off coefficient, NPV was also decreased from approximately 70 $mm to over 65 $mm as NPV was decreased by only around 5 $mm. This is because the greater leak-off coefficient characteristics have a considerable influence on the fluid volume requirement, and it impacts on reducing fracture geometry and increase in the total treatment cost [10], and it returns to sharply reduce NPV. Thus, NPV is vastly decreased with increasing leak-off coefficient from 0.003 ft/min$^{0.5}$ and 0.005 ft/min$^{0.5}$. However, NPV is slowly decreased with increasing leak-off coefficient from 0.005 ft/min$^{0.5}$ to 0.007 ft/min$^{0.5}$.

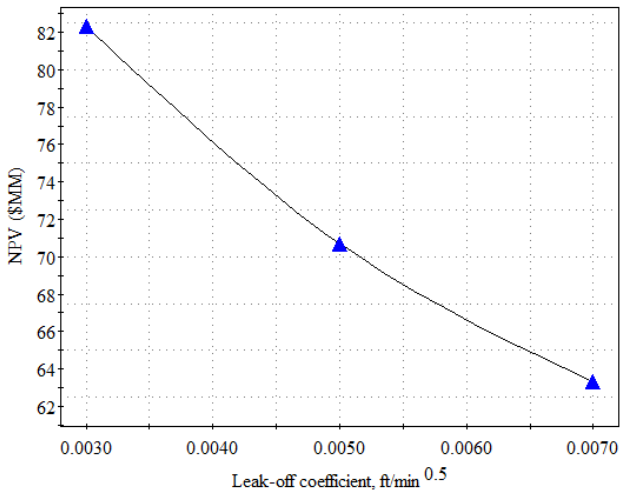

Figure-10. Effect of leak coefficient on NPV.

5.3 The Effect of Pump Rate on Net Present Value (NPV)

Figure-11 shows the pump rate of hydraulic fracturing versus the net present value. There is a linear trend relationship between pump rate and net present value. In addition, Figure-11 is noticeable that the net present value increases from 62 $mm to 78 $mm as the pump rate increases from 16 bpm to 30 bpm. Between 16 bpm to 23 bpm of pump rate, NPV increases from 62 $mm to nearly 71 $mm, and it increases by nearly 9 $mm. between 23 bpm to 30 bpm of pump rate, NPV also increases by nearly 8 $mm. Thus, NPV increases in all cases of pump rate because the pump rate is increased with increasing fracture width and net pressure. This is due to the pump rate directly proportional to the net pressure and fracture width, leading to an increased fracture conductivity, and it returns to NPV. However, the design pump rate cannot be increased by more than 30 bpm because it must be ensured that the bottom treating pressure was not exceeded the burst pressure of production tubing size 2-7/8in in the properties of tubing grade C-75, nominal weight 6.5 ppf, burst pressure resistance of 9,910 psi [15] and the design pump rate is above 16 bpm because it must be ensured that the bottom hole treating pressure

initially creates net pressure to propagates fracture width and length and proppant transport.

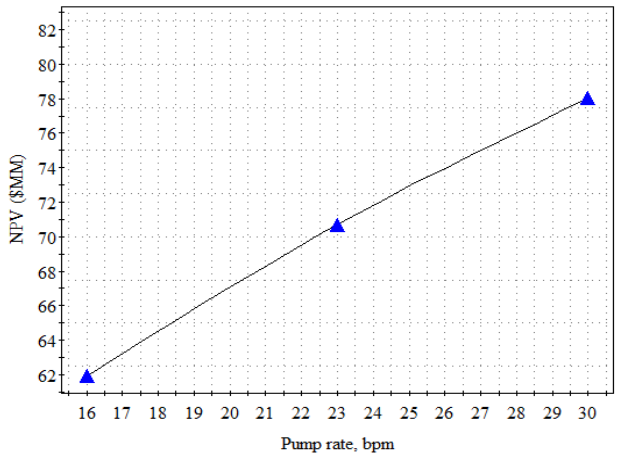

Figure-11. Effect of pump rate on NPV.

5.4 The Effect of Proppant Concentration on Net Present Value (NPV)

It is noticeable that there is a nonlinear trend relationship between NPV and proppant concentration. Figure-12 shows that the NPV increases slightly from over 68 $mm to over 72 $mm when the proppant concentration increases from 6 ppg to 10 ppg [11]. This is because proppant concentration directly increases the fracture conductivity as it increases the propped width and packed proppant permeability, and it turns to an increase in NPV, which exceeds an increase in the proppant cost [16]. However, the design proppant concentration cannot be increased by more than 10 ppg because it must be ensured that the total friction pressure is constrained within 100 psi to 300 psi [17, 18] and it also must be prevented the tip screen issue during injecting proppant slurry. In addition, the design proppant concentration is above 6 ppg to ensure that the proppant distribution in the fractures area is always above 0.5 lb/ft^2 [17]

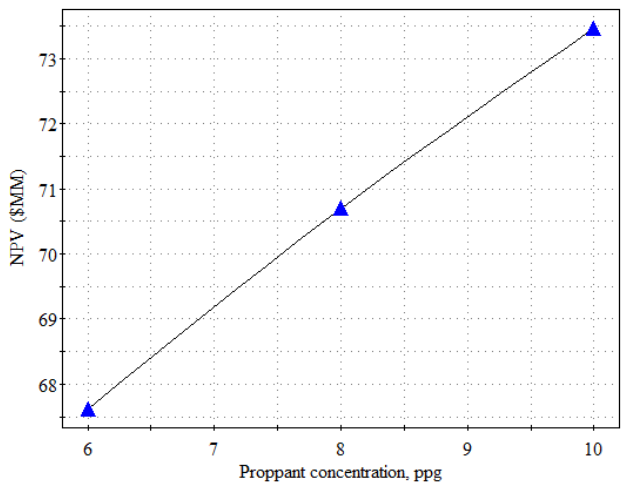

Figure-12. Effect of proppant concentration end of the job on NPV.

5.5 The Effect of Injection Time on Net Present Value (NPV)

Figure-13 shows NPV versus injection time. It is noticeable that there is a slight linear trend between injection time and NPV. It also shows that NPV sharply increases between over 67.5 $mm to nearly 73.4 $mm as the injection time increases from 60 minutes to 90 minutes. This is because an increase in injection time is directly proportional to an increase in total slurry volume requirement as it increases the fracture volume, and it turns to an increase in NPV [16].

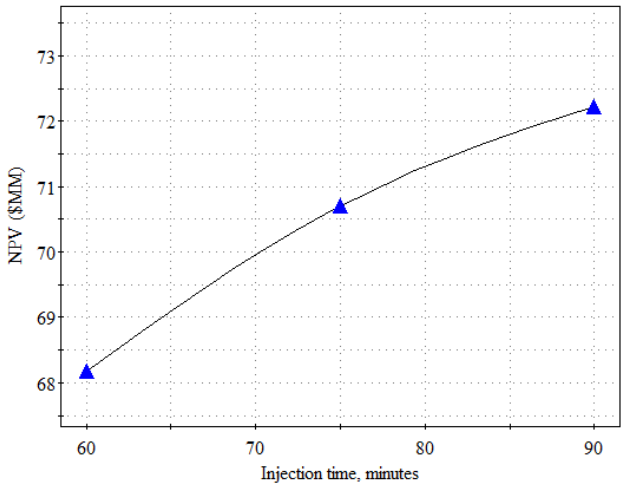

Figure-13. Effect of injection time on NPV.

5.6 The Effect of Porosity of the Reservoir on the Net Present Value (NPV)

Several literatures presented the influence of porosity on production performance. Reservoir properties such as thickness, porosity, and oil saturation had a larger effect on production performance than flow properties (permeability, viscosity, oil API, and reservoir pressure) [19]. In this study, the formation porosity was evaluated from 14% to 24% of the lower Miocene formation. Figure-14 shows that the NPV increases following a linear trend as the porosity of the reservoir increases from 14% to 24% in all cases, and in turn increases the oil recovery factor [20, 21, 22].

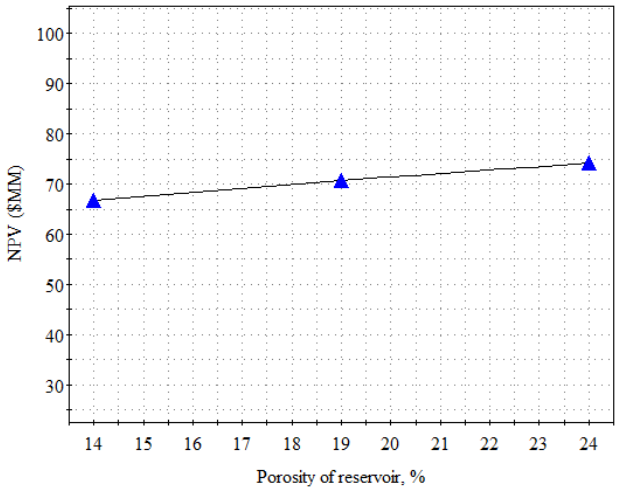

Figure-14. Effect of porosity of reservoir on NPV.

5.7 The Effect of the Net Pay Thickness on Net Present Value (NPV)

Figure-15 presents that the reservoir thickness is an important factor that significantly influences the production performance (NPV). In addition, previous literature published that an increase in oil production was noticeable with an increased thickness of the reservoir Amjed Hassan *et al*. [23]. Figure-15 shows that there is a nonlinear between the net present value and reservoir thickness. This Figure studies that NPV increases considerably from over 25 $mm to over 100 $mm as the reservoir thickness increases between 30 ft to 230 ft. Thus, the reservoir thickness strongly effects on NPV because it increases the conductivity, and it turns to increase the production performance.

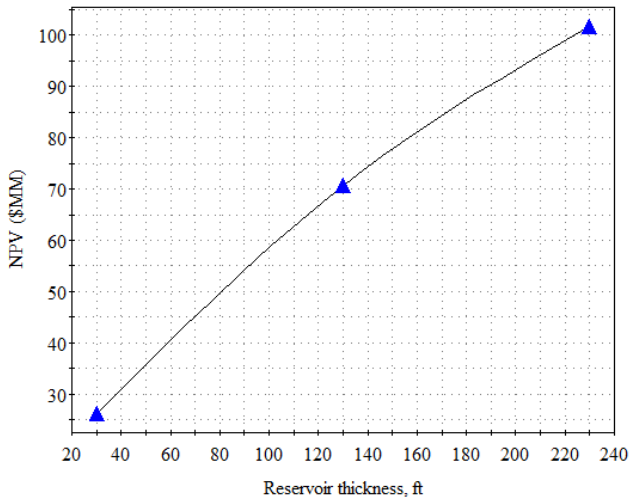

Figure-15. Effect of reservoir thickness on NPV.

CONCLUSIONS

The study on the effects of treatment design parameters on enhanced oil production in the Lower Miocene formation using Box-Behnken design could be summarized as follows:

- The NPV is significantly increased with increasing the net pay thickness within 30 ft to 230 ft.
- The NPV is considerably decreased with increasing the leak-off coefficient within 0.003 ft/min$^{0.5}$ to 0.007 ft/min$^{0.5}$.
- The interaction between treatment design parameters and porosity of reservoir and the net pay thickness have been discussed in this study.

ACKNOWLEDGEMENT

This research is funded by Petrovietnam University under the grant code of GV2006.

REFERENCES

[1] Michael Economides, Ronald Oligney and Peter Valko. 2002. Unified Fracture Design. Orsa Press Alvin, Texas.

[2] Robert S. Schechter. 1991. Oil well stimulation. Prentice Hall.

[3] Queipo N. V., Verde A. J., Canelon J. and Pintos S. 2002. Efficient global optimization for hydraulic fracturing treatment design. J. Pet. Sci. Eng. 35:151-166.

[4] 2003. User guide to Modde. Umetrics AB version 7.0.

[5] Valko P. and Economides M. J. 1995. Hydraulic Fracture Mechanics. Chichester, England: John Wiley and Sons.

[6] Ferreira S. L. C., Bruns R. E., Ferreira H. S., Matos G. D., David J. M., Brando G. C. *et al.* 2007. Box - Behnken design: An alternative for the optimization of analytical methods. Analytica Chimica Acta, 597(2): 179-186.

[7] Box G. E. P. and Wilson K. B. 1951. On the experimental attainment of optimum conditions. Journal of the Royal Statistical Society. 13(1): 1-45.

[8] Sun Y., Li T., Yan I. and Lin J. 2010. Technology optimization for polysaccharides (POP) extraction from the fruiting. bodies: of Pleurotus ostreatus by Box -- Behnken statistical design. Carbohydrate Polymers. 80(1): 242-247. SPE 20670.

[9] Ngoc T. B. Nguyen, Cuong T. Q. Dang, Wisup Bae, Taemoon Chung. 2010. Integrating Geological Characterization and Historical Production Analysis to Optimize Field Management of Lower Miocene Reservoir in White Tiger Field, Vietnam. SPE Journal. Of Canadian Petroleum Technology.

[10] Meng H.-Z and Brown K. E. 1987. Coupling of production forecasting, fracture geometry requirements and treatment scheduling in the optimum hydraulic fracture design. SPE 16435, Low Permeability Reservoirs Symposium, Denver, CO.

[11] M. M. Rahman, M. K. Rahman and S. S. Rahman. 2003. Optimizing treatment parameters for enhanced hydrocarbon production by hydraulic fracturing. Journal of Canadian Petroleum Technology.

[12] Jain S., Prestride A., Dellorusso P., Nguyen N. C., Duong L.D., Vu H.Q. 2007. Case Study from 12 Successful Years of High Temperature Fracturing in Bach Ho Field Offshore Viet Nam. The 2007 SPE Production and Operations Symposium at Oklahoma, USA, 31 March - 3 April, SPE 106712.

[13] Vogel J. V. 1968. Inflow performance relationships for solution gas drive wells. J. Petroleum Technology.

[14] Hagedorn and Brown. 1965. Experimental study of pressure gradients occurring, during continuous two-phase flow in small-diameter conduits. J. Petroleum Technol. 475.

[15] 2005. API Specification 5CT Eighth Edition, July 1.

[16] M. M. Rahman *et al*. 2007. Multicriteria Hydraulic Fracturing Optimization for Reservoir Stimulation. Petroleum Science and Technology.

[17] Michael J. 2007. Economides, Tony Martin. Modern hydraulic fracturing.

[18] John L. Gidley *et al*. 1989. Recent Advances in Hydraulic Fracturing. Society of Petroleum Engineers Richardson, TX.

[19] Llaguno P. E., Moreno F, Gracia R. and Méndez Escobar E. 2002. A Reservoir Screening Methodology for SAGD Applications. Paper 2002-124, CIPC, Calgary Canada, June.

[20] Susmit Chakraborty *et al*. 2000. Numerical Modeling on the Influence of Reservoir Porosity and Microbial Kinetics on Enhanced Oil Recovery by Microbial Flooding. SPE-200639-MS.

[21] R. Alcantara *et al.* 2017. Applications of Material Balance for Determining the Dynamic Performance of Fractures in a Dual Porosity System in HP-HT Reservoirs. SPE-187694-MS.

[22] S. Rezaei-Gomari and F. Amrouche. 2017. Investigating the Effect of Rock Pore Size Distribution on Reservoir Production Performance. ICCM, Guilin, Guangxi, China.

[23] Amjed Hassan *et al*. 2000. Effect of Formation Damage, Length and Reservoir Thickness on the Inflow Performance of Horizontal Wells. URTEC-2021-5486-MS.

[24] Nguyen Huu Truong, Ha Nhu Y. 2021. Applications of response surface methodology and Box-Behnken Design to Optimise fracture treatment design for Lower Miocene reservoirs, Bach Ho Field. Petrovietnam Journal, Vol 5.